THE JOURNAL OF BIOLOGICAL CHEMISTRY VOL. 288, NO. 29, pp. 21389–21398, July 19, 2013

Activation of the Transcription Factor GLI1 by WNT Signaling Underlies the Role of SULFATASE 2 as a Regulator of Tissue Regeneration*[S]

Received for publication, December 31, 2012, and in revised form, June 4, 2013 Published, JBC Papers in Press, June 5, 2013, DOI 10.1074/jbc.M112.443440

Ikuo Nakamura[‡1], Maite G. Fernandez-Barrena[§1], Maria C. Ortiz-Ruiz[¶], Luciana L. Almada[§], Chunling Hu[‡], Sherine F. Elsawa[‖], Lisa D. Mills[§], Paola A. Romecin[¶], Kadra H. Gulaid[‡], Catherine D. Moser[‡], Jing-Jing Han[§], Anne Vrabel[§], Eric A. Hanse[**], Nicholas A. Akogyeram[‡], Jeffrey H. Albrecht[**], Satdarshan P. S. Monga[‡‡], Schuyler O. Sanderson[§§], Jesus Prieto[¶¶], Lewis R. Roberts[‡2], and Martin E. Fernandez-Zapico[‡§3]

From the [‡]Division of Gastroenterology and Hepatology, Mayo Clinic and Mayo Clinic Cancer Center, Rochester, Minnesota 55905, the [§]Schulze Center for Novel Therapeutics and [§§]Department of Laboratory Medicine and Pathology, Mayo Clinic, Rochester, Minnesota 55905, the [¶]Departamento de Fisiología Facultad de Medicina Universidad de Murcia, 30100 Murcia, Spain, the [‖]Department of Biological Sciences, Northern Illinois University, Illinois 60115, the [**]Division of Gastroenterology, Hennepin County Medical Center, Minneapolis, Minnesota 55404, the [‡‡]Departments of Pathology and Medicine, University of Pittsburgh School of Medicine, Pittsburgh, Pennsylvania 15216, and the [¶¶]Centro de Investigacion Medica Aplicada, 31008 Pamplona, Spain

Background: Tissue regeneration is a complex process involving a network of ligand-activated pathways.
Results: The sulfatase SULF2 modulates cell proliferation and organ growth through a WNT-dependent activation of the transcription factor GLI1.
Conclusion: Together, these data define a novel cascade regulating tissue regeneration.
Significance: The knowledge derived from this study will contribute to the understanding of the molecular mechanisms modulating regeneration and organogenesis.

Tissue regeneration requires the activation of a set of specific growth signaling pathways. The identity of these cascades and their biological roles are known; however, the molecular mechanisms regulating the interplay between these pathways remain poorly understood. Here, we define a new role for SULFATASE 2 (SULF2) in regulating tissue regeneration and define the WNT-GLI1 axis as a novel downstream effector for this sulfatase in a liver model of tissue regeneration. SULF2 is a heparan sulfate 6-*O*-endosulfatase, which releases growth factors from extracellular storage sites turning active multiple signaling pathways. We demonstrate that SULF2-KO mice display delayed regeneration after partial hepatectomy (PH). Mechanistic analysis of the SULF2-KO phenotype showed a decrease in WNT signaling pathway activity *in vivo*. In isolated hepatocytes, SULF2 deficiency blocked WNT-induced β-CATENIN nuclear translocation, TCF activation, and proliferation. Furthermore, we identified the transcription factor GLI1 as a novel target of the SULF2-WNT cascade. WNT induces GLI1 expression in a SULF2- and β-CATENIN-dependent manner. GLI1-KO mice phenocopied the SULF2-KO, showing delayed regeneration and decreased hepatocyte proliferation. Moreover, we identified CYCLIN D1, a key mediator of cell growth during tissue regeneration, as a GLI1 transcriptional target. GLI1 binds to the *cyclin d1* promoter and regulates its activity and expression. Finally, restoring GLI1 expression in the liver of SULF2-KO mice after PH rescues CYCLIN D1 expression and hepatocyte proliferation to wild-type levels. Thus, together these findings define a novel pathway in which SULF2 regulates tissue regeneration in part via the activation of a novel WNT-GLI1-CYCLIN D1 pathway.

Regulation of tissue regeneration involves the ligand-dependent activation of multiple growth factor pathways (1–4). Release from extracellular storage is one of the most frequent mechanisms modulating the activity of these ligands (5). The SULFATASE 2 (SULF2)[4] is a heparan sulfate (HS) endosulfatase enzyme that removes 6-*O*-sulfate moieties from disaccharide units in HS proteoglycans (HSPGs) (6, 7). HSPGs are present on the cell surface and in the extracellular matrix of virtually all animal cells and act both as storage or sequestration sites for growth factors and as co-receptors in growth factor-receptor interactions (5). The storage and co-receptor activities of HSPGs are dependent on the sulfation state of the HS polymers (5, 8). The enzymatic removal of 6-*O*-sulfate by SULF2 regulates binding of growth factors to HS, and therefore has significant effects on the local extracellular concentration and activ-

* This work was supported, in whole or in part, by National Institutes of Health Grants CA100882 and CA128633 (to L. R. R.) and CA165076 (to L. R. R. and M. E. F.-Z.); the Mayo Clinic Center for Cell Signaling in Gastroenterology (NIDDK P30DK084567) (to M. E. F.-Z.); the Mayo Clinic Cancer Center (CA15083), the Mayo Clinic Center for Translational Science Activities (National Institutes of Health/NCRR CTSA Grant KL2 RR024151), and an American Gastroenterological Association Foundation for Digestive Health and Nutrition Bridging Grant (to L. R. R.).
[S] This article contains supplemental Figs. S1–S4.
[1] Both authors contributed equally to this work.
[2] To whom correspondence may be addressed. E-mail: roberts.lewis@mayo.edu.
[3] To whom correspondence may be addressed. E-mail: fernandezzapico.martin@mayo.edu.

[4] The abbreviations used are: SULF2, SULFATASE 2; PH, partial hepatectomy; NT, non-targeting control; shRNA, small hairpin RNA; RT-PCR, reverse transcriptase-PCR; HS, heparan sulfate; HSPG, heparan sulfate proteoglycan; BrdU, bromodeoxyuridine.

ity of a number of heparan sulfate-binding growth factors (8–12). In this study, we used liver after partial hepatectomy (PH) as a model of tissue regeneration. This model has been extensively characterized at the biological level, and the kinetics of cell proliferation, and activation of ligands and pathways involved in the process of liver regeneration post-hepatectomy are well known (1–4, 16). However, the molecular mechanisms regulating the interplay between these ligand-activated pathways and the downstream effectors remain elusive.

Here, we demonstrate that SULF2 expression is elevated during the early stages of liver regeneration after PH, and that its loss decreases cellular proliferation and impairs tissue regeneration. Analysis of the mechanism identifies a novel WNT-GLI1 axis as a downstream effector for this sulfatase. SULF2-KO mice show a decrease in WNT pathway activity *in vivo* and *in vitro* after PH. Expression studies demonstrate that the transcription factor GLI1 is a novel transcriptional target of the SULF2-WNT cascade. GLI1 belongs to the GLI family of transcription factors, which are known effectors of different developmental-regulated pathways such as the HEDGEHOG pathway (13–14). Similar to SULF2-KO, GLI1-KO mice show delayed liver regeneration after PH. In isolated hepatocytes, GLI1 knockdown decreases proliferation and CYCLIN D1 expression. Further, we identified CYCLIN D1 as a transcriptional target of GLI1 downstream of WNT3a. GLI1 binds to the *cyclin d1* promoter and regulates its expression *in vitro* and *in vivo*. Finally, using a transposase-based transfection system combined with hydrodynamic delivery of the expression vectors, we restored GLI1, and rescued CYCLIN D1 expression and hepatocyte proliferation in the SULF2-KO liver after PH. Together, these results demonstrate a novel role for SULF2 in tissue regeneration and define the WNT-GLI1 pathway as an effector of this phenomenon.

EXPERIMENTAL PROCEDURES

Animals—SULF2-KO mice (strain name: B6;129P2-*Sulf2 Gt(pGT1TMpfs)1Ucd*) created by gene trap insertional mutagenesis were obtained from the Mutant Mouse Regional Resource Center at University of California, Davis, stock number 0403-UCD. Mice were maintained in a temperature-controlled (22 °C), pathogen-free environment and fed a standard rodent chow diet and water *ad libitum*. All mice were on a mixed 129 × C57BL/6 genetic background. SULF2-KO mice were crossed with B6.129 mice as recommended by Jackson Labs, and WT littermates were used as controls. The care and use of the animals for the studies at Mayo Clinic were reviewed and approved by the Institutional Animal Care and Use Committee at Mayo Clinic. For the GLI1 knock-out mouse (GLI1-KO) experiment, C57BL/6 WT and GLI1-KO mice (15) on the B6 background were raised and maintained in the animal facilities of the University of Murcia (Murcia, Spain). All experimental procedures at the University of Murcia were performed according to Spanish and European Community guidelines for the use of experimental animals.

Partial Hepatectomy (PH)—For experimental procedures, mice were anesthetized with ketamine (100 mg/kg of body weight) plus xylazine (10 mg/kg of body weight) by intraperitoneal injection. A standard 70% PH was performed according to Higgins and Anderson (16). In WT, and SULF2-KO, five to ten animals in each cohort were sacrificed at 0, 0.5, 1, 3, 6, 12, 24 (1 day), 36, 48 (2 days), 72 (3 days), 120 (5 days), 168 (7 days), and 240 h (10 days) post-PH. Animals were injected with 50 mg/kg bromodeoxyuridine (BrdU, Roche, Indianapolis, IN) 2 h before sacrifice at the indicated postoperative time points with the exception of 7 and 10 days. In WT or GLI1-KO mice, PH ($n = 3$) was performed and mice were sacrificed at 24 h (1 day), and 96 h (4 days). At the time of sacrifice, mice were anesthetized, and the remaining liver lobes were removed. Resected liver tissue was weighed and frozen in liquid nitrogen for later analysis. The liver to body weight ratio was calculated as liver weight (g) ×100/body weight (g). Part of each liver sample was also fixed in 10% formalin, embedded in paraffin, and stained with hematoxylin-eosin (H&E) for histological analysis by an expert liver pathologist. Survival rates after partial hepatectomy were 100% for WT, SULF2-KO, and GLI1-KO mice.

Hydrodynamic Injection—In this protocol, animals received tail vein injections containing two constructs. One construct contains a GLI1-transposon, and the other is a sleeping beauty transposase. Both constructs were injected in a 2:1 molar ratio (17). Plasmids were prepared using Qiagen (Valencia, CA) EndoFree Maxi DNA Kit and resuspended in lactated ringers at a final volume 10% the weight of the animal and injected via tail vein in <10 s, through a 27 gauge, 0.5 inch needle. A total of 25 μg of plasmid were used for the injections (18). The animals were placed in a restraining device for the injections.

Primary Hepatocyte Culture, BrdU Incorporation, and Wnt3a Treatment—Primary hepatocytes were isolated from WT and SULF2-KO mouse livers using collagenase perfusion and Percoll gradients, as previously described (19). Cells were cultured on collagen-treated plastic plates in Williams E medium. The medium was changed daily. Four hours after the isolation of hepatocytes, the medium was changed, and cells were either transfected with control siRNA, siRNA targeting β-CATENIN or vectors expressing either non-targeting (NT) shRNA or shRNA targeting GLI1 (11, 20). Transfection of isolated mouse hepatocytes was performed using Fugene 6 transfection reagent (Roche Diagnostics GmbH, Mannheim, Germany) following the manufacturer's protocol. Forty-eight hours after transfection, mouse WNT3a (1324-WN, R&D Systems, Minneapolis, MN) (5 ng/ml) was added to serum-free media. Similar experiments were done using GLI1-expressing plasmid DNA or control vector (pCMV-3XFlag, Sigma-Aldrich). Cell proliferation was measured in cultured hepatocytes using the BrdU incorporation assay at 6, 12, 24, and 48 h after addition of WNT3a. Each experiment was performed in six replicates at least three times. Total RNA and protein lysates were prepared from hepatocyte cultures as described previously (11).

Chemicals, Plasmids, and Antibodies—Cyclopamine was purchased from Toronto Research Chemicals (Toronto, Canada). Mouse SHH ligand was obtained from R&D Systems. Cell Proliferation Labeling Reagent (RPN201) and anti-BrdU antibody (RPN202) were from GE Healthcare UK Limited (Buckinghamshire, UK), Vector M.O.M. Peroxidase Kit (PK-2200, Vector laboratories Inc, Burlingame, CA), and rabbit polyclonal anti-β-CATENIN antibody (sc-1496R, Santa Cruz Biotechnology, Santa Cruz, CA) were used for immunohistochemistry. The following antibodies were used for immunoblotting: CYCLIN D1 (06-137,

Upstate Cell Signaling, Temecula, CA), β-ACTIN (A5316, Sigma-Aldrich), WNT3a (ab19925, Abcam, Cambridge, MA), β-CATENIN (9582, Cell Signaling Technology Inc, Danvers, MA), and LAMIN B (sc-6216, Santa Cruz Biotechnology). NE-PER nuclear and cytoplasmic extraction reagents (D8835, Thermo Scientific, Rockford, IL), protease inhibitor mixture set III (539134, Calbiochem, San Diego, CA), PVDF membrane (IPVH00010, Millipore), 4–15% Tris HCl gels (Bio-Rad), and ECL-enhanced chemiluminescence reagents (Denville Scientific Inc., Metuchen, NJ) were used for immunoblotting. Trizol (Invitrogen, Carlsbad, CA), RNeasy Mini Kit (Qiagen, Valencia, CA), and SuperScript III First-Strand Synthesis System (Invitrogen) were used for real-time polymerase chain reaction (real-time PCR). The following primers for real-time PCR were purchased from Applied Biosystems (Foster City, CA): mouse GLI1 (Mm00494646), mouse GLI2 (Mm01293117), mouse GLI3 (Mm01165737), mouse PTCH1 (Mm01306906), mouse SULFATASE 1 (SULF1) (Mm00552283), mouse SULF2 (Mm01248029), mouse CYCLIN D1 (Mm00432359), mouse GLUTAMINE SYNTHETASE (GS) (Mm00725701), mouse 18S (Mm03928990), human GLI1 (Hs01110766), and human 18S (Hs99999901). SYBR Green PCR Master Mix was purchased from Bio-Rad (170-8880). Control siRNA (sc-37007) and siRNA targeting β-CATENIN (sc-44253) were from Santa Cruz Biotechnology. Constructs expressing NT sequences or shRNA targeting GLI1 were previously described (20). TOPFLASH (TCF binding site TK-luciferase reporter) plasmids were obtained from Dr. Wanguo Liu as previously described (11, 21). The GLI-luciferase reporter was kindly provided by Dr. Chi-chung Hui (University of Toronto, Toronto, Ontario, Canada), and the sleeping beauty and parental transposon vectors were provided by Dr. Karl Clark (Department of Biochemistry and Molecular Biology, Mayo Clinic, Rochester, MN). The GLI1-containing transposon construct was cloned into the pKT2C-mC vector using standard recombinant DNA methodology (20). For the chromatin immunoprecipitation (ChIP) assay, the EZ-Magna ChIP G kit (17-409, Millipore, Billerica, MA) was used. GLI1 (2553) and TCF4 (2569) antibodies were obtained from Cell Signaling and normal rabbit IgG from Millipore (12-370).

Immunohistochemistry—To assess cell proliferation, BrdU labeling was used to identify cells undergoing DNA synthesis in the S-phase of the mitotic cycle. Immunohistochemical detection of BrdU was performed using anti-BrdU antibody as described previously (11). For β-CATENIN immunohistochemistry, rabbit polyclonal anti-β-CATENIN antibody (1:600) was used. Visualization was carried out using Rabbit on Rodent HRP-polymer (50-832-78, Fisher Scientific) followed by incubation with diaminobenzidine (Sigma-Aldrich). Sections were counterstained with hematoxylin (GHS132-1L, Sigma-Aldrich). BrdU- and β-CATENIN-positive nuclei were counted in five 400× fields on each slide (positive nuclei/total nuclei).

Western Blot—Whole liver protein lysates were prepared in lysis buffer as previously described (11). Nuclear proteins were prepared using the NE-PER nuclear and cytoplasmic protein isolation kit (Thermo Scientific) according to the manufacturer's protocol. Equal amounts of protein (50 μg/lane) were separated by electrophoresis on a 4–15% Tris HCl gel and then transferred to PVDF membrane. Blots were probed with polyclonal or monoclonal antibodies against CYCLIN D1 (1:1000), WNT3a (1 μg/ml), β-ACTIN (1:2000), or β-CATENIN (1:1000). The Western blots shown are representative samples from at least five (maximum of ten) animals in each group. The membranes were scanned and the density of the protein bands was analyzed with Bio-Rad densitometry software Molecular Analyst.

Tissue Culture—The L3.6 cell line was kindly provided by Dr. Fidler (MD Anderson Cancer Center, Houston, TX). WT MEFs were a gift from Dr. John Hawse (Mayo Clinic, Rochester, MN) and were cultured in DMEM supplemented with 10% FBS. AML12 and HepG2 cell lines were obtained from American Type Culture Collection (ATCC) (Manassas, VA) and cultured as previously described (11, 20).

Luciferase Assay—Cell lines and isolated hepatocytes from WT and SULF2-KO mice, plated onto 24-well plates at a density of 6×10^4 cells per well, were allowed to adhere overnight. On the following day, the cells were transfected with the TOPFLASH reporter construct (0.025 μg/well) or GLI-luciferase reporter (0.1 μg/well) and then serum-starved in medium overnight, followed by treatment with mouse WNT3a ligand for the indicated times. Samples were harvested and prepared for luciferase assays following the manufacturer protocol (Promega, Madison, WI). To control for intersample variations in transfection efficiency, the total protein for the samples in each well was quantitated using the Bio-Rad protein assay, and luciferase readouts were normalized to protein content. Relative luciferase represents luciferase readouts/protein concentration normalized to control cells within each experiment.

Chromatin Immunoprecipitation (ChIP) Assay—ChIP assay was performed following the EZ-Magna ChIP kit protocol. Briefly, AML12 cells (10×10^6) were cross-linked with 1% formaldehyde for 10 min at room temperature. The cells were then washed and scraped with phosphate-buffered saline and collected by centrifugation at $800 \times g$ for 5 min at 4 °C, resuspended in cell lysis buffer, and incubated on ice for 15 min. The pellet was then resuspended in nuclear lysis buffer and sheared to fragment DNA to ~400 bp. Chromatin samples were either aliquoted as genomic input DNA or immunoprecipitated using 1 μg of TCF4 or GLI1 antibodies or normal rabbit IgG, overnight at 4 °C on a rotating wheel. Following immunoprecipitation, samples were washed and eluted using the chromatin immunoprecipitation kit. Cross-links were removed at 65 °C for 5 h. DNA was purified using spin columns. Semi-quantitative PCR of the ChIP products and genomic input DNA was performed. PCR products were visualized in 2% agarose gel. PCR primers were designed flanking the TCF4 consensus sequences in the mouse *gli1* promoter: *gli1*-F (5′-tggcctgagagatctgtttaag-3′) and *gli1*-R (5′-ctgcgtgagctcaaagaaac-3′). For the mouse *cyclin D1* ChIP the following primers were used to amplify the area containing GLI biding sites: *cyclin D1*-F (5′-taggaaggagcctatcgtgtctca-3′) and *cyclin D1*- R (5′-caacagctcaagatggtggccatt-3′).

RNA Isolation and Real-time PCR Analysis—Total RNA was prepared from liver tissue, and cell lines using Trizol, followed by cleanup using the RNeasy Mini Kit. The SuperScript III First-Strand Synthesis System was used for the production of complementary DNA. For quantitative real-time PCR analysis, primers for SULF1, SULF2, GLI1, 2, 3, GS, CYCLIN D1, and

PTCH1 were used in an ABI 7900 system with the following profile: 95 °C for 10 min followed by 40 cycles of 15 s at 95 °C and 60 s at 60 °C. To analyze the expression levels of mouse CD36, samples for quantitative PCR were prepare with 1X SYBR Green PCR Master Mix and the following primers: CD36, 5′-gatgacgtggcaaagaacag-3′ (forward) and 5′-tcctcggggtcctgagttat-3′ (reverse); 18S, 5′-aacccgttgaaccccattcgtgat-3′ (forward) and 5′-caggttcacctacggaaaccttgt-3′ (reverse). Amplification was performed using the C1000 Thermal Cycler (Bio-Rad) under the following reaction conditions: 95 °C for 3 min followed by 40 cycles of 30 s at 95 °C, 30 s at 60 °C and 20 s at 72 °C. Each mRNA level was normalized by comparison to 18S ribosomal RNA levels in the same samples. The results were calculated following the 2ΔCp method.

Liver Triglyceride Content Determination—Liver triglycerides were extracted and measured using a Triglyceride Quantification Kit (ab65336, Abcam). Briefly, frozen liver tissue samples were homogenized in a 1 ml solution containing 5% Nonidet P-40 in water, then slowly heated to 80–100 °C in a water bath for 5 min and subsequently cooled to room temperature. This process was repeated twice. After centrifugation to remove any insoluble material, samples were diluted 10-fold with distilled water. Finally, samples were prepared following the manufacturer's protocol and quantitated using a colorimetric assay.

Statistical Analysis—All data represent at least five (maximum of ten) independent mice and are expressed as the mean ± S.E. Differences between groups were compared using a two-tailed Student's *t* test. One-way ANOVA was used to compare samples from the different time points in the same group.

RESULTS

Loss of SULF2 Delays Liver Regeneration After PH—First, we determined whether the physiological stimulus of PH influences SULF2 expression in WT mice. The SULF2 mRNA level increased by 3 h and peaked at 24 h after PH compared with the level at 0 h (supplemental Fig. S1*A*). Next, we performed PH on WT and SULF2-KO mice. The ratio of liver to body weight was used to determine the degree of liver growth after resection. At baseline, the liver/body ratio was not significantly different in SULF2-KO compared with WT mice. However, 7 days after PH, the liver/body weight ratio of SULF2-KO mice was significantly decreased by 14.8% compared with that of WT mice (data not shown). H&E-stained sections show no major abnormalities in the livers of SULF2-KO compared with WT mice at baseline. Microvesicular steatosis, a well-known histopathological feature present during regeneration after PH (22–27), was seen in both WT and SULF2-KO mouse livers beginning at 12 h after PH. However, 48 h after PH, SULF2-KO mice showed a decrease in microvesicular steatosis compared with WT mice. This decrease in microvesicular formation correlated with decreased levels of hepatic triglyceride content (supplemental Fig. S2*A*) and mRNA expression levels of the lipid translocase CD36, an established marker of lipogenesis during liver regeneration (26) (supplemental Fig. S2*B*). Furthermore, 10 days post PH, microvesicular steatosis had resolved as expected in WT mice, but it persisted in the livers of SULF2-KO mice (Fig. 1*A*).

To determine whether SULF2 is required for hepatocyte proliferation in the regenerating mouse liver, we assessed cell proliferation in WT and SULF2-KO mice by examining BrdU incorporation as well as by counting mitotic figures. The levels and kinetics of BrdU incorporation and mitosis in WT mice were similar to previously published reports of the PH model (1–4, 28–31) (Fig. 1, *B* and *C*). The percentage of BrdU-positive hepatocyte nuclei in SULF2-KO mice was significantly lower than the percentage observed in WT mice from 36 to 72 h after PH (Fig. 1*B*), as was the number of hepatocyte mitoses at 48 h (Fig. 1*C*). Finally, we measured the levels of the cell cycle regulator CYCLIN D1, a well-established regulator of cell growth known to be up-regulated during liver regeneration (28, 29). The induction of CYCLIN D1 expression was significantly decreased in SULF2-KO mice at 36 and 48 h after PH (Fig. 1*D*). These results demonstrate a role for SULF2 in liver regeneration and suggest an underlying mechanism in the regulation of hepatocyte proliferation by this sulfatase.

SULF2 Deficiency Down-regulates WNT/β-CATENIN Pathway Activity After PH—WNT signaling pathway is induced at early stages of liver regeneration within hours after hepatectomy, and it plays a key role in the regulation of this cellular process (30, 31). Blockade of the pathway by inactivation of β-CATENIN, a downstream effector of the cascade, delays liver regeneration after PH in mice. Overexpression of constitutively active mutant β-CATENIN accelerates this process (24, 25). Immunohistochemical analysis shown in Fig. 2*A* (*left panel*) demonstrates increased nuclear β-CATENIN after PH; however, SULF2-KO mice showed significantly lower expression of nuclear β-CATENIN at 3 h post PH compared with WT littermates (Fig. 2*A*, *right panel*). To confirm the downstream effect of SULF2-KO on WNT signaling, we measured the expression of the β-CATENIN target gene *glutamine synthetase* (*gs*) (34). SULF2-KO and WT mice expressed similar levels of GS mRNA at 0 h. However by 6 h post PH, the expression of GS was 2.2-fold higher in WT mice, while SULF2-KO mice levels remained the same (Fig. 2*B*).

To further define the role of this SULF2-WNT/β-CATENIN signaling during liver regeneration, we determined whether primary hepatocytes isolated from SULF2-KO mice displayed decreased baseline or WNT-induced nuclear β-CATENIN and cell proliferation rates when compared with hepatocytes from WT mice. SULF2 deficiency in hepatocytes inhibits the activation of WNT/β-CATENIN signaling by WNT3a, a ligand of the pathway induced at early stages during PH (supplemental Fig. S3). Measurement of nuclear β-CATENIN by immunoblotting following densitometry showed that loss of SULF2 inhibited the WNT3a-induced increase in nuclear β-CATENIN after WNT treatment (Fig. 2*C*). The baseline incorporation of BrdU in primary mouse hepatocytes lacking SULF2 was 35% lower than in hepatocytes from WT mice (Fig. 2*D*). Further, hepatocytes from SULF2-KO mice were insensitive to WNT3a stimulation of cell proliferation (Fig. 2*D*). Next, we assessed activation of WNT3a-induced WNT/β-CATENIN signaling by transfection of the TOPFLASH plasmid vector that contains multiple WNT-sensitive TCF binding sites driving luciferase expression in primary hepatocytes isolated from WT or SULF2-KO mice. SULF2 deficiency decreased TCF-driven TOPFLASH lucifer-

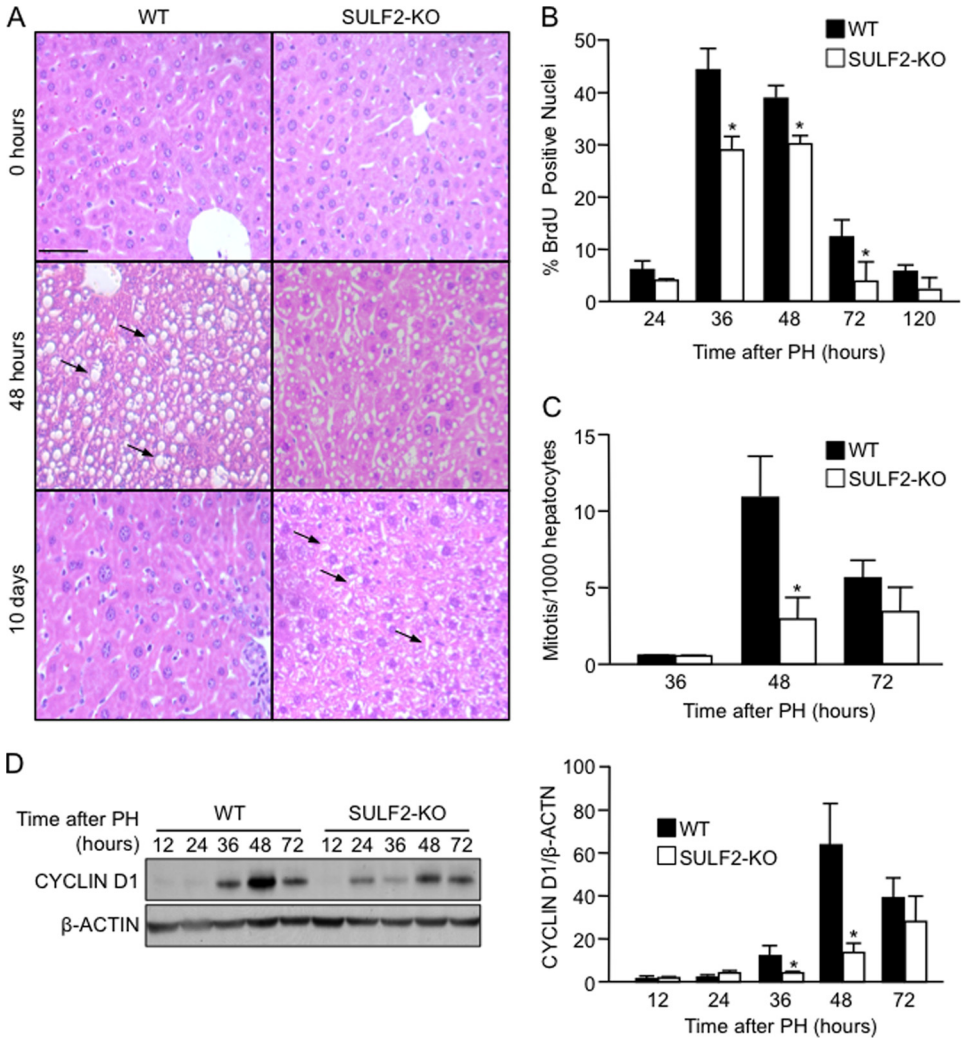

FIGURE 1. **Liver regeneration is delayed in SULFATASE 2 (SULF2)-KO mice after PH.** *A*, formalin-fixed paraffin-embedded sections were stained using hematoxylin-eosin. Photomicrographs were taken at ×400 magnification. The scale bar is a 100 μm in length. SULF2-KO mice show less steatosis (*arrows*) than WT mice at 48 h after PH, but steatosis (*arrows*) persists longer in the SULF2-KO compared with the WT mice, in which steatosis has almost completely resolved by 10 days after PH. *B*, decreased percentage of BrdU-positive nuclei in livers of SULF2-KO mice compared with WT mice 36, 48, and 72 h after PH (*, $p < 0.05$). *C*, decreased mitotic index in the livers of SULF2-KO mice compared with WT mice at 48 h after PH (*, $p < 0.05$). All data shown are representative of five to ten mice per genotype per time point and are presented as mean ± S.E. *D*, CYCLIN D1 expression after PH is significantly suppressed and delayed in SULF2-KO mice, as shown by Western blot analysis (*left panel*). β-ACTIN was used as the loading control for the densitometry analysis (*right panel*) (*, $p < 0.05$).

ase activity by 88% at 6 h after treatment (Fig. 2*E*). Conversely, overexpression of SULF2 in HepG2 liver cells resulted in an almost 10-fold increase in TOPFLASH reporter activity (Fig. 2*F*). Thus, SULF2 deficiency not only decreases the intrinsic replicative capacity of hepatocytes but also makes them substantially less responsive to the proliferative effects of WNT signaling activation.

GLI1 Is a Direct Transcriptional Target of the WNT/β-CATENIN Pathway—Expression studies searching for target genes regulated by the WNT/β-CATENIN pathway during PH identified the transcription factor GLI1 as candidate mediator of the cellular effect of this cascade. There was a statistically significant decrease in GLI1 expression in the liver of SULF2-KO animals compared with WT mice 6 h post PH (Fig. 3*A*). There were no changes in the expression of the other members of the GLI family of transcription factors, GLI2 and GLI3, suggesting that this is an effect specific to GLI1 (Fig. 3*B*). Next, we investigated whether GLI1 expression can be regulated by the SULF2-WNT axis. We measured the expression of GLI1 after WNT3a stimulation of primary hepatocytes isolated from WT and SULF2-KO mice. Baseline GLI1 mRNA expression was lower in hepatocytes from SULF2-KO mice than in WT mice (Fig. 3*C*, 0 min). Remarkably, WNT3a treatment increased GLI1 mRNA expression in hepatocytes isolated from WT mice at 60 and 120 min after treatment. In contrast, hepatocytes isolated from SULF2-KO mice were completely unresponsive to WNT3a treatment, and GLI1 mRNA levels did not increase (Fig. 3*C*). Next, we examined whether the WNT3a ligand functionally regulates GLI1-mediated transcription using a reporter vector containing 8 consecutive GLI1 binding sites upstream of the luciferase gene. WNT3a treatment upregulated GLI1-mediated luciferase activity in hepatocytes from WT mice (Fig. 3*D*). Similar results were obtained using HepG2 cells or AML12 immortalized mouse hepatocytes (supplemental Fig. 4*A* and data not shown). However, baseline GLI-mediated luciferase activity was almost completely inhibited in

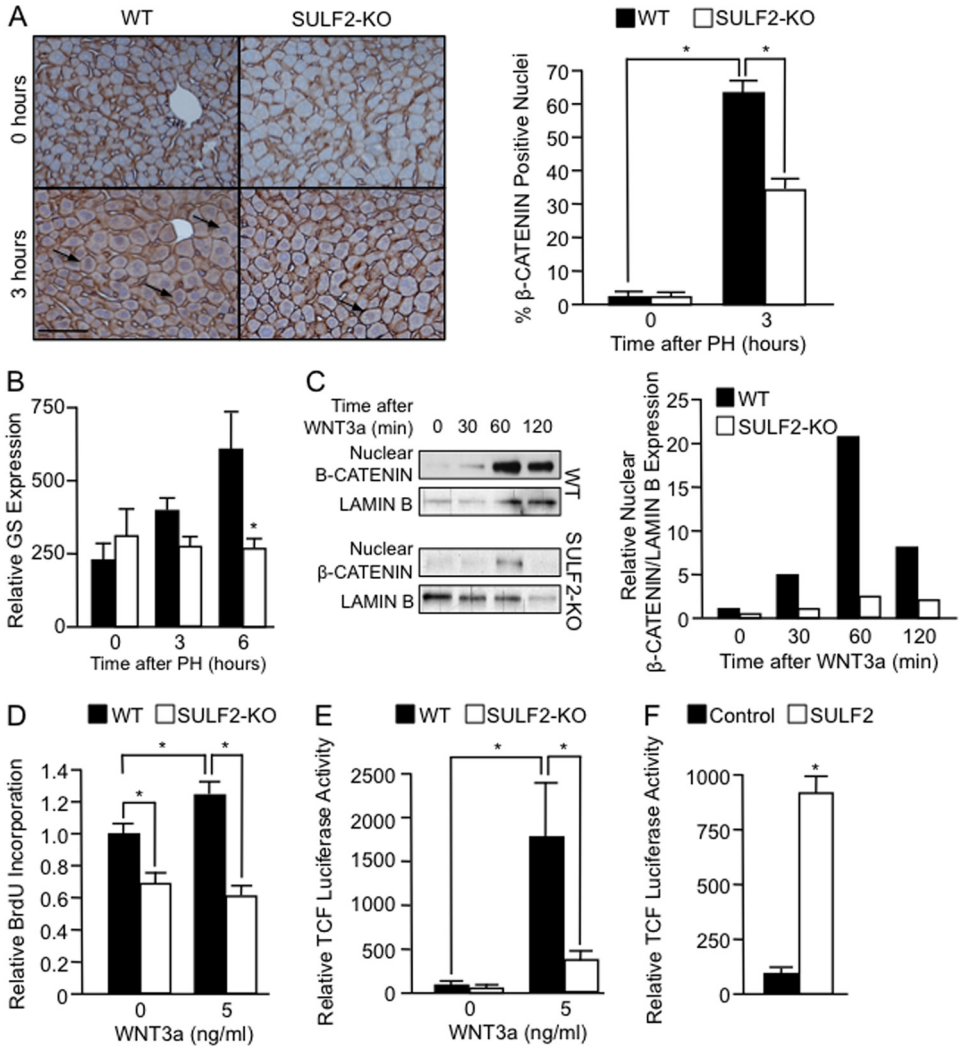

FIGURE 2. **Loss of SULF2 impairs WNT pathway activity *in vitro* and *in vivo*.** *A*, immunohistochemical detection of β-CATENIN show decreased nuclear levels in liver from SULF2-KO mice compared with WT mice after PH. The graph shows the quantitation of nuclei positive for β-CATENIN at baseline and 3 h post PH (see *black arrows*) (*, $p < 0.01$). The scale bar is a 100 μm in length. *B*, decreased expression of the mRNA for the WNT/β-CATENIN target gene *glutamine synthetase* (*gs*) in the livers of SULF2-KO mice compared with WT mice after PH as assessed by real-time PCR (*, $p < 0.05$). Each mRNA level was normalized to 18S levels in the same samples. Data shown in *panels A* and *B* are representative of five to ten mice per genotype per time point and are presented as mean ± S.E. *C*, substantially decreased WNT3a-induced nuclear β-CATENIN in isolated hepatocytes from SULF2-KO mice compared with WT mice as measured by Western blot analysis (*left panel*). LAMIN B was used as the loading control for the densitometry analysis (*right panel*). *D*, BrdU incorporation analysis shows decreased baseline and WNT3a-induced proliferation of hepatocytes isolated from SULF2-KO mice compared with WT mice (*, $p < 0.01$). *E*, decreased WNT3a-induced TCF-mediated TOPFLASH luciferase activity in isolated hepatocytes from SULF2-KO mice compared with WT mice. The experiments were repeated at least three times with similar results. *F*, reporter luciferase assay shows that similar to WNT3a treatment the overexpression of SULF2 significantly (*, $p < 0.01$) increases TOPFLASH reporter activity in HepG2 liver cells.

hepatocytes isolated from SULF2-KO mice, and the cells were resistant to WNT3a-stimulation (Fig. 3*D*). Finally, we demonstrate that overexpression of SULF2 increases GLI-mediated transcription in AML12 cells (Fig. 3*E*).

To determine whether the effect of WNT on GLI1 mRNA expression was mediated through the canonical WNT/β-CATENIN pathway, we examined the effect of siRNA-mediated knockdown of β-CATENIN expression on GLI1 mRNA levels in isolated hepatocytes. Transfection of hepatocytes with siRNA targeting β-CATENIN resulted in a substantial reduction in total cellular β-CATENIN in hepatocytes from WT mice (Fig. 4*A*, *inset*) and significantly decreased GLI1 mRNA levels (Fig. 4*A*). *In silico* analysis of the mouse *gli1* promoter showed the presence of two canonical TCF binding sequences near the transcriptional initiation sites (data not shown). To confirm whether WNT3a-induced transcriptional activity regulates the *gli1* promoter through the WNT/β-CATENIN pathway transcription factor TCF4, we performed a ChIP assay using sheared chromatin from AML12 cells. As shown in Fig. 4*B*, endogenous TCF4 binds to a region −4,295 to −4,078 bp upstream of the transcriptional start site in the *gli1* promoter.

Next, we examined whether this WNT regulatory effect was independent of HEDGEHOG, the most well characterized modulator of GLI transcription factor expression and activity during cell proliferation (13, 14). Isolated hepatocytes from WT mice did not show differences in cell proliferation (supplemental Fig. S4*B*) or expression of GLI1 (Fig. 4*C*) after treatment with the HEDGEHOG inhibitor, Cyclopamine. Treatment with this inhibitor did not affect the induction of GLI transcriptional activity by SULF2 (Fig. 4*D*). In addition, SONIC HEDGEHOG

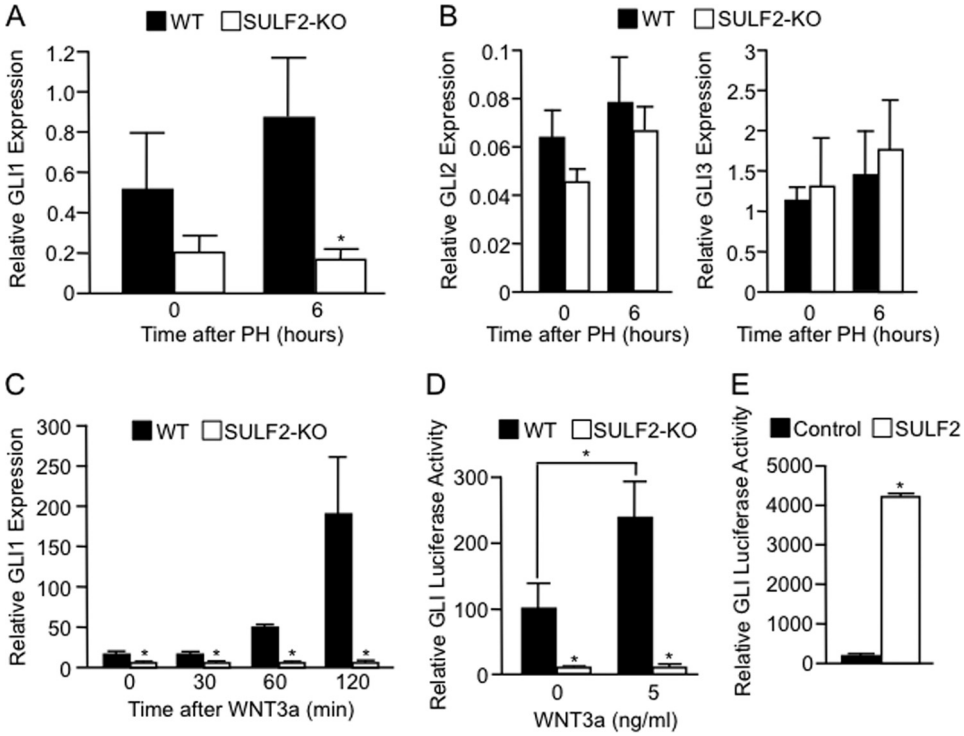

FIGURE 3. **SULF2 is required by WNT3a to induce GLI1 expression.** *A*, mRNA expression of GLI1 in SULF2-KO mice was decreased compared with WT mice at baseline and also at 6 h after PH (*, $p < 0.01$). *B*, qPCR analysis shows no changes in the expression of GLI2 and GLI3 after PH. *C*, expression of GLI1 mRNA increased after WNT3a treatment in WT hepatocytes, but GLI1 mRNA did not increase its expression in SULF2-deficient hepatocytes treated WNT3a (*, $p < 0.01$ at all the indicated timepoints). *B-C*, data were normalized to 18S RNA expression. *D*, GLI1 transcriptional activity was measured by transfecting a luciferase-expressing construct regulated by a promoter containing 8 consecutive GLI1 binding sites and measuring luciferase activity in lysates from hepatocytes treated with WNT3a at concentration of 5 ng/ml for 24 h. WNT3a induces the activity of this reporter in WT hepatocytes, this effect was substantially blunted in hepatocytes from SULF2-KO mice (*, $p < 0.001$). Data shown are representative of three samples per genotype per time point and are presented as mean ± S.E. *E*, similar to WNT3a treatment, SULF2 overexpression induces GLI1 activity in mouse immortalize hepatocyte line AML12 (*, $p < 0.05$).

(SHH), a ligand of the HEDGEHOG pathway, did not induce GLI1 expression in AML12 cells (supplemental Fig. S4*C*, *left panel*). As a control for the SHH activation of the pathway, we used mouse embryonic fibroblast (MEF), cells known to be SHH responsive. In these cells, the ligand increases the expression of GLI1 (supplemental Fig. S4*C*, *right panel*) to a level similar to ones already reported (35). Finally, we demonstrate that the activity of the HEDGEHOG pathway was not significantly affected at the early stages of liver regeneration in SULF2-KO mice. As shown in Fig. 4*E*, the mRNA levels of PTCH1, a marker of the activity of this cascade (14), did not change post PH. Together, these results support a HEDGEHOG-independent regulation of GLI1 by the canonical WNT/β-CATENIN/TCF4 pathway.

GLI1 Regulates Hepatocyte Proliferation, and Its Loss Results in Delayed Liver Regeneration after PH—To further determine whether the effects of the SULF2-WNT axis on hepatocyte proliferation are mediated through GLI1, we investigated the effects of changes in GLI1 levels with respect to hepatocyte proliferation. WT hepatocytes that were transfected with an shRNA construct targeting GLI1 showed a decrease in BrdU incorporation (Fig. 5*A*). Conversely, GLI1 overexpression increased BrdU incorporation in WT hepatocytes compared with vector-transfected cells (Fig. 5*B*). Expression controls for the efficiency of GLI1 overexpression and shRNA targeting are shown in supplemental Fig. S4*D*.

Next, we reasoned that if the effect of SULF2-WNT activation on liver regeneration is mediated through GLI1, then loss of GLI1 should phenocopy the SULF2-KO. To determine whether GLI1 is required for liver regeneration, a PH was performed on GLI1-KO mice. Starting at 24 h post PH, the liver/body weight ratio of GLI1-KO mice was significantly lower than that of WT mice. At 96 h, the GLI1-KO mice present with ~20% reduction in the liver/body ratio compared with the WT mice (data not shown). This result suggests that similar to the effect of SULF2 deficiency, GLI1 deficiency significantly delays liver regeneration post PH supporting the role of these molecules as part of the same signaling axis.

Further analysis of the mechanism identified CYCLIN D1 as a direct target of GLI1 in hepatocytes. Similar to the SULF2-KO mice, the induction of CYCLIN D1 was impaired in GLI1-KO mice after PH (Fig. 5*C*). Bioinformatics analysis demonstrates the presence of three candidate GLI binding sites (G) in the mouse *cyclin d1* promoter (Fig. 5*D*). In Fig. 5*E* we show the direct binding of endogenous GLI1 to a region located −812 and −612 bp upstream of the transcription start site in the mouse *cyclin d1* promoter. Further, transfection of mouse GLI1 increased *cyclin d1* promoter activity and expression in AML12 cells (Fig. 5*F*).

Finally, to define the role of GLI1 as an effector of SULF2-WNT axis, we rescued the expression of GLI1 in SULF2-KO mice using hydrodynamic delivery of GLI1 and control vectors. These constructs were stably transfected in the liver using a transposase-based system (17). Data included in Fig. 6 show that restoring GLI1 expression to WT levels rescues the levels of CYCLIN D1 in SULF2-KO mice after PH (Fig. 6*A*). In addi-

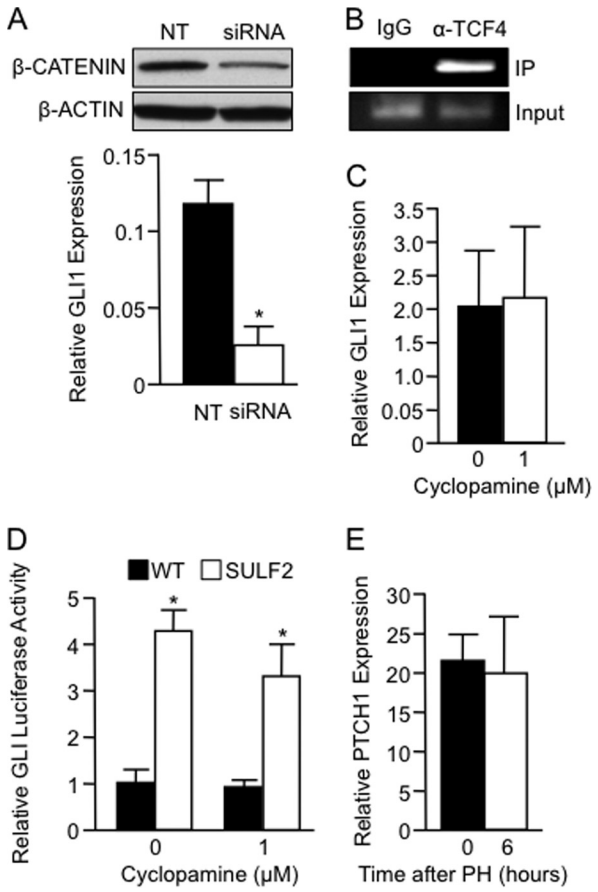

FIGURE 4. **WNT regulates GLI1 expression through the canonical pathway in a HEDGEHOG-independent manner.** *A*, siRNA mediated knockdown of *β*-CATENIN significantly decreased GLI1 mRNA expression in hepatocytes isolated from WT mice (*, $p < 0.05$). Efficiency of the knockdown was determined by Western blot (see *inset*). *B*, ChIP assay shows binding of endogenous TCF4 to the *gli1* promoter in AML12 cells. *C*, relative GLI1 expression in isolated hepatocytes form WT mice show that the treatment with HEDGEHOG inhibitor, Cyclopamine, did not affect the levels of this transcription factor. GLI1 mRNA level was normalized to 18S levels in the same samples. *D*, similarly, induction of GLI1 transcriptional activity by SULF2 in L3.6 cells was not affected by the treatment with the Cyclopamine. Overexpression of SULF2 induces GLI1 transcriptional activity even in the presence of this inhibitor (*, $p < 0.05$). *E*, HEDGEHOG pathway was not significantly affected in SULF2-KO mice as shown by the mRNA expression of PTCH1, a marker for the activity of the pathway.

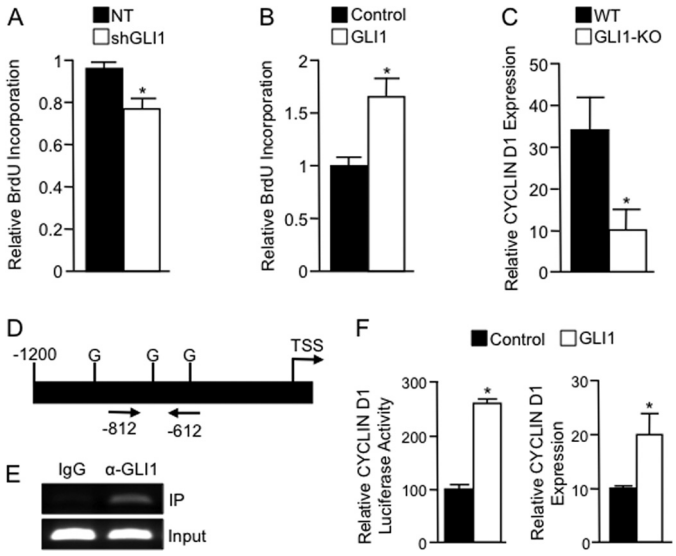

FIGURE 5. **GLI1 regulates liver regeneration and hepatocyte proliferation.** *A*, BrdU incorporation was measured in isolated mouse hepatocytes after transfection of the NT control or shRNA targeting GLI1. Knockdown of GLI1 decreased proliferation as shown by the decrease in BrdU levels (*, $p < 0.05$). *B*, conversely, overexpression of GLI1 increased the incorporation of BrdU in hepatocytes from WT mice (*, $p < 0.05$). *C*, CYCLIN D1 mRNA levels were increased after 24 h after PH, this effect was impaired in GLI1-KO mice. mRNA levels were assessed by qPCR and normalized to mouse 18S levels. *D*, *in-silico* analysis show the presence of 3 GLI binding site (G) in the mouse *cyclin d1* promoter upstream of the transcription start site (TSS). *E*, endogenous GLI1 binds to the mouse promoter in AML12 cells. Positive amplicon for the ChIP assay is marked between *arrows* (−812/−612 bp). *F*, reporter assay and qPCR analysis show increase activity of the mouse *cyclin d1* promoter and expression in AML12 cells overexpressing GLI1 (*, $p < 0.05$).

tion, the proliferative capacity of the regenerating liver measured by BrDU incorporation shows similar levels in WT and SULF2-KO livers transfected with GLI1 (Fig. 6*B*-C). Together these findings define a novel role for GLI1 in the regulation of cell proliferation and tissue regeneration, and identify the SULF2-WNT pathway as a regulator of this transcription factor and its target gene, *cyclin d1*.

DISCUSSION

This study identified a novel SULF2-WNT-GLI1 pathway involved in the regulation of early stages of liver regeneration (Fig. 6*D*). We made the following key observations: 1) knock-out of SULF2 delays liver regeneration after PH; 2) knock-out of SULF2 down-regulates WNT pathway signaling during liver regeneration after PH; 3) the WNT3a proliferative response in hepatocytes involves the up-regulation of GLI1; 4) knock-out of GLI1 also delays liver regeneration after PH and acts as an effector of this SULF2-WNT axis; and 5) CYCLIN D1 is a direct transcriptional target of the SULF2-WNT-GLI1 pathway.

SULF1 and SULF2 are the known members of the heparan sulfate endosulfatase family. Although SULF1 and SULF2 both desulfate HSPGs by removing 6-O-sulfates from mature HS chains and appear to show redundancy in certain effects, they do not have completely overlapping effects. *In vivo* experiments using the double SULF1/SULF2-KO demonstrate a functional cooperation at the level of 6-*O*-sulfation where HS is significantly higher than in mice with knock-out of either SULF1 or SULF2 (7, 36). We have observed that liver regeneration is delayed in the absence of SULF2, but it eventually recovers without an apparent contribution of SULF1. We measured the SULF1 mRNA levels in both WT and SULF2-KO mice after PH. The level of SULF1 in both WT and SULF2-KO mice increased 1.5 fold after PH, peaking at 24 h; however, no significant difference was noted in SULF1 mRNA between WT and SULF2-KO mice at any individual time point (supplemental Fig. 1*B*). Thus, SULF2 deficiency is not accompanied by a major compensatory increase in SULF1 expression during liver regeneration. The factors determining the selective role of SULF2 in this cellular process will require further exploration.

The accumulation of hepatocellular fat ("transient steatosis") occurring in the liver after PH is known to play a role in the regenerative response (22–24). This accumulation is concomitant with hepatocyte proliferation, and it can contribute to the regulation cell growth (23). Blockade of hepatic fat accumulation after PH using pharmacological and genetic means causes inhibition of liver regeneration (24, 27). Lipids are used as an

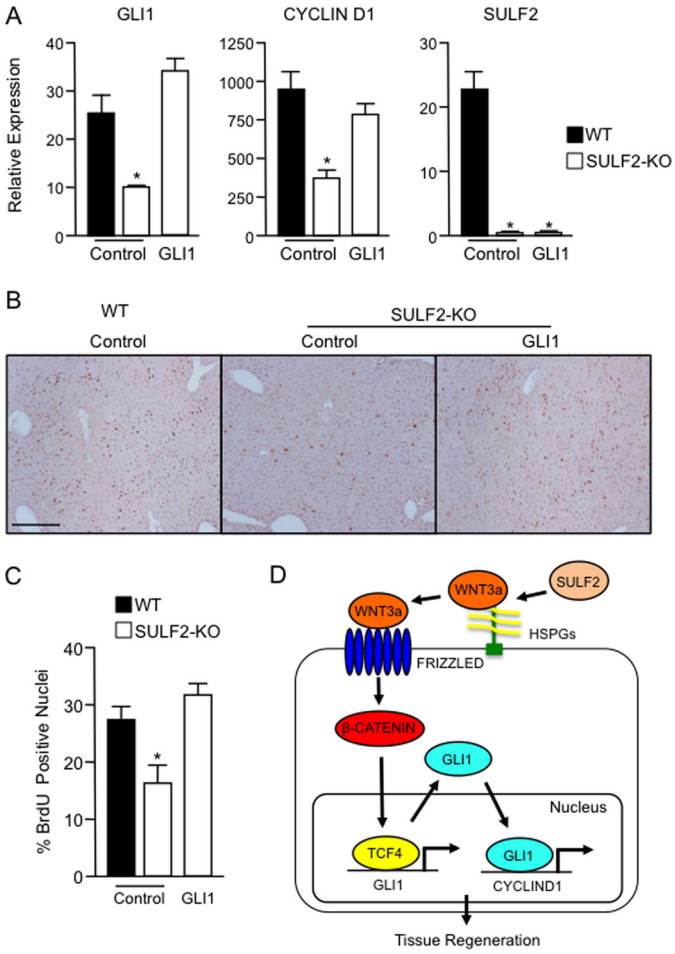

FIGURE 6. **GLI1 can rescue SULF2 deficiency during liver regeneration.** *A*, mRNA expression of GLI1, CYCLIN D1, and SULF2 was measured in WT and SULF2-KO transfected with either empty vector or GLI1-expressing construct. qPCR analysis shows that restoration of GLI1 expression rescue CYCLIN D1 expression to the WT levels (*, $p < 0.05$). The data were normalized to 18S expression. *B–C*, BrdU incorporation was measured as described under "Experimental Procedures" in liver 48 h after PH. The percentage of BrdU-positive nuclei in livers of SULF2-KO mice transfected with GLI1 expression constructs is higher that control transfected SULF2-KO mice (*, $p < 0.05$). *D*, schematic representation of this novel WNT pathway downstream of SULF2 involved in the regulation of gene expression and tissue regeneration.

energy source by the hepatocyte for DNA replication and phospholipids synthesis. The most important source of lipids that accumulates in the regenerating liver is mainly free fatty acids supplied from adipose tissue. However, *de novo* hepatic fatty acid synthesis has also been reported (26). According to these observations, our study shows a delay in fat accumulation that is accompanied by a delay in cell proliferation. These data suggest that SULF2 may play additional roles in the regulation of cell growth independent of the regulation of CYCLIN D1, and may involve the modulation of lipid accumulation in the liver.

Previous studies show that mice with conditional knock-out of β-CATENIN in hepatocytes display suboptimal regeneration or delayed onset of regeneration. Additionally, they exhibit a biphasic trend in proliferation that peaked at day 3 and increased slightly again at day 14 (32, 33). We found that SULF2-KO significantly delayed liver regeneration post PH. The delay in liver regeneration correlates with decreased translocation of β-CATENIN to the hepatocyte nuclei, thus suggesting that SULF2 regulates liver regeneration in part through effects on the WNT/β-CATENIN signaling pathway (Fig. 2). In addition, we have identified a novel regulatory mechanism for CYCLIN D1 in this cellular process. This mechanism involves the transcription factor GLI1 acting downstream of β-CATENIN, thus expanding the repertoire of transcriptional regulators controlled by this pathway.

The WNT/β-CATENIN and HEDGEHOG signaling pathways are important in the coordination of developmental transitions and have been postulated to interact at multiple levels (37–39). However, these interactions have not been completely elucidated. We found that SULF2 deficiency substantially inhibits the WNT/β-CATENIN signaling pathway post PH, resulting in lower expression of GLI1. Interestingly, hepatocytes isolated from WT mice treated with WNT3a show an increase in GLI1 expression, and SULF2 is necessary for WNT induction of GLI1 in a HEDGEHOG-independent manner. Similar to the SULF2-KO, GLI1-KO also delayed liver regeneration after PH suggesting that WNT/β-CATENIN signaling regulates GLI1, and GLI1 plays an important role in liver regeneration. Finally, we demonstrate that this axis acts on the cell cycle regulator CYCLIN D1. In SULF2-KO and GLI1-KO mice the levels of CYCLIN D1 are lower compared with WT controls. GLI1 binds to the promoter of *cyclin d1* and regulates the expression of this cyclin and the activity of its promoter. Additional experiments beyond the scope of this study are needed to investigate the epigenetics mechanism regulated by GLI1 and define the possible interplay between HEDGEHOG signaling and SULF2/GLI1 in cells having both pathways active.

In summary, our results show that SULF2-WNT3a-GLI1 regulates liver regeneration after PH through activation of the WNT/β-CATENIN signaling pathway, and consequent downstream activation of GLI1 by regulating CYCLIN D1 (Fig. 6*D*). Together these findings provide new insight into the mechanisms controlling liver regeneration and could serve as a foundation for the development of novel therapeutic regimens aimed at improving tissue regeneration.

Acknowledgments—We thank the Microarray Core Facility at Mayo Clinic for technical assistance with real-time PCR, Jennifer L. Rud for secretarial assistance, Kimberly K. McGee for editorial assistance, and Lucas P. Nacusi, Suresh K. Nayar, and Gregory J. Gores for critical review of the manuscript.

REFERENCES

1. Borowiak, M., Garratt, A. N., Wüstefeld, T., Strehle, M., Trautwein, C., and Birchmeier, C. (2004) Met provides essential signals for liver regeneration. *Proc. Natl. Acad. Sci. U.S.A.* **101,** 10608–10613
2. Monga, S. P., Pediaditakis, P., Mule, K., Stolz, D. B., and Michalopoulos, G. K. (2001) Changes in WNT/beta-catenin pathway during regulated growth in rat liver regeneration. *Hepatology* **33,** 1098–1109
3. Ochoa, B., Syn, W. K., Delgado, I., Karaca, G. F., Jung, Y., Wang, J., Zubiaga, A. M., Fresnedo, O., Omenetti, A., Zdanowicz, M., Choi, S. S., and Diehl, A. M. (2010) Hedgehog signaling is critical for normal liver regeneration after partial hepatectomy in mice. *Hepatology* **51,** 1712–1723
4. Natarajan, A., Wagner, B., and Sibilia, M. (2007) The EGF receptor is required for efficient liver regeneration. *Proc. Natl. Acad. Sci. U.S.A.* **104,** 17081–17086
5. Kirkpatrick, C. A., and Selleck, S. B. (2007) Heparan sulfate proteoglycans

at a glance. *J. Cell Sci.* **120**, 1829–1832
6. Frese, M. A., Milz, F., Dick, M., Lamanna, W. C., and Dierks, T. (2009) Characterization of the human sulfatase Sulf1 and its high affinity heparin/heparan sulfate interaction domain. *J. Biol. Chem.* **284,** 28033–28044
7. Lamanna, W. C., Frese, M. A., Balleininger, M., and Dierks, T. (2008) Sulf loss influences N-, 2-O-, and 6-O-sulfation of multiple heparan sulfate proteoglycans and modulates fibroblast growth factor signaling. *J. Biol. Chem.* **283,** 27724–27735
8. Ai, X., Do, A. T., Kusche-Gullberg, M., Lindahl, U., Lu, K., and Emerson, C. P., Jr. (2006) Substrate specificity and domain functions of extracellular heparan sulfate 6-O-endosulfatases, QSulf1 and QSulf2. *J. Biol. Chem.* **281,** 4969–4976
9. Lai, J. P., Sandhu, D. S., Yu, C., Han, T., Moser, C. D., Jackson, K. K., Guerrero, R. B., Aderca, I., Isomoto, H., Garrity-Park, M. M., Zou, H., Shire, A. M., Nagorney, D. M., Sanderson, S. O., Adjei, A. A., Lee, J. S., Thorgeirsson, S. S., and Roberts, L. R. (2008) Sulfatase 2 up-regulates glypican 3, promotes fibroblast growth factor signaling, and decreases survival in hepatocellular carcinoma. *Hepatology* **47,** 1211–1222
10. Viviano, B. L., Paine-Saunders, S., Gasiunas, N., Gallagher, J., and Saunders, S. (2004) Domain-specific modification of heparan sulfate by Qsulf1 modulates the binding of the bone morphogenetic protein antagonist Noggin. *J. Biol. Chem.* **279,** 5604–5611
11. Lai, J. P., Oseini, A. M., Moser, C. D., Yu, C., Elsawa, S. F., Hu, C., Nakamura, I., Han, T., Aderca, I., Isomoto, H., Garrity-Park, M. M., Shire, A. M., Li, J., Sanderson, S. O., Adjei, A. A., Fernandez-Zapico, M. E., and Roberts, L. R. (2010) The oncogenic effect of sulfatase 2 in human hepatocellular carcinoma is mediated in part by glypican 3-dependent Wnt activation. *Hepatology* **52,** 1680–1689
12. Lemjabbar-Alaoui, H., van Zante, A., Singer, M. S., Xue, Q., Wang, Y. Q., Tsay, D., He, B., Jablons, D. M., and Rosen, S. D. (2010) Sulf-2, a heparan sulfate endosulfatase, promotes human lung carcinogenesis. *Oncogene* **29,** 635–646
13. Hui, C. C., and Angers, S. (2011) Gli proteins in development and disease. *Annu. Rev. Cell Dev. Biol.* **27,** 513–537
14. Stecca, B., Ruiz, I., and Altaba, A. (2010) Context-dependent regulation of the GLI code in cancer by HEDGEHOG and non-HEDGEHOG signals. *J. Mol. Cell. Biol.* **2,** 84–95
15. Park, H. L., Bai, C., Platt, K. A., Matise, M. P., Beeghly, A., Hui, C. C., Nakashima, M., and Joyner, A. L. (2000) Mouse Gli1 mutants are viable but have defects in SHH signaling in combination with a Gli2 mutation. *Development* **127,** 1593–1605
16. Higgins, G. M., and Anderson, R. M. (1931) *Arch. Pathol.* **12,** 186–202
17. Geurts, A. M., Yang, Y., Clark, K. J., Liu, G., Cui, Z., Dupuy, A. J., Bell, J. B., Largaespada, D. A., and Hackett, P. B. (2003) Gene transfer into genomes of human cells by the sleeping beauty transposon system. *Mol. Ther.* **8,** 108–117
18. Liang, K. W., Nishikawa, M., Liu, F., Sun, B., Ye, Q., and Huang, L. (2004) Restoration of dystrophin expression in mdx mice by intravascular injection of naked DNA containing full-length dystrophin cDNA. *Gene Ther.* **11,** 901–908
19. Gumucio, J. J., May, M., Dvorak, C., Chianale, J., and Massey, V. (1986) The isolation of functionally heterogeneous hepatocytes of the proximal and distal half of the liver acinus in the rat. *Hepatology* **6,** 932–944
20. Elsawa, S. F., Almada, L. L., Ziesmer, S. C., Novak, A. J., Witzig, T. E., Ansell, S. M., and Fernandez-Zapico, M. E. (2011) GLI2 transcription factor mediates cytokine cross-talk in the tumor microenvironment. *J. Biol. Chem.* **286,** 21524–21534
21. Liu, W., Dong, X., Mai, M., Seelan, R. S., Taniguchi, K., Krishnadath, K. K., Halling, K. C., Cunningham, J. M., Boardman, L. A., Qian, C., Christensen, E., Schmidt, S. S., Roche, P. C., Smith, D. I., and Thibodeau, S. N. (2000) Mutations in AXIN2 cause colorectal cancer with defective mismatch repair by activating beta-catenin/TCF signalling. *Nat. Genet.* **26,** 146–147
22. Delahunty, T. J., and Rubinstein, D. (1970) Accumulation and release of triglycerides by rat liver following partial hepatectomy. *J. Lipid Res.* **11,** 536–543
23. Michalopoulos, G., Cianciulli, H. D., Novotny, A. R., Kligerman, A. D., Strom, S. C., and Jirtle, R. L. (1982) Liver regeneration studies with rat hepatocytes in primary culture. *Cancer Res.* **42,** 4673–4682
24. Shteyer, E., Liao, Y., Muglia, L. J., Hruz, P. W., and Rudnick, D. A. (2004) Disruption of hepatic adipogenesis is associated with impaired liver regeneration in mice. *Hepatology* **40,** 1322–1332
25. Yu, S., Matsusue, K., Kashireddy, P., Cao, W. Q., Yeldandi, A. V., Rao, M. S., Gonzalez, F. J., and Reddy, J. K. (2003) Adipocyte-specific gene expression and adipogenic steatosis in the mouse liver due to peroxisome proliferator-activated receptor γ1 (PPARγ1) overexpression. *J. Biol. Chem.* **278,** 498–505
26. Rudnick, D. A., and Davidson, N. O. (2012) Functional relationships between lipid metabolism and liver regeneration. *Int. J. Hepatol.* **2012,** 1–8
27. Walldorf, J., Hillebrand, C., Aurich, H., Stock, P., Hempel, M., Ebensing, S., Fleig, W. E., Seufferlein, T., Dollinger, M. M., and Christ, B. (2010) Propranolol impairs liver regeneration after partial hepatectomy in C57Bl/6-mice by transient attenuation of hepatic lipid accumulation and increased apoptosis. *Scand. J. Gastroenterol.* **45,** 468–476
28. Hanse, E. A., Mashek, D. G., Becker, J. R., Solmonson, A. D., Mullany, L. K., Mashek, M. T., Towle, H. C., Chau, A. T., and Albrecht, J. H. (2012) Cyclin D1 inhibits hepatic lipogenesis via repression of carbohydrate response element binding protein and hepatocyte nuclear factor 4α. *Cell Cycle* **11,** 2681–2690
29. Hanse, E. A., Nelsen, C. J., Goggin, M. M., Anttila, C. K., Mullany, L. K., Berthet, C., Kaldis, P., Crary, G. S., Kuriyama, R., and Albrecht, J. H. (2009) Cdk2 plays a critical role in hepatocyte cell cycle progression and survival in the setting of cyclin D1 expression *in vivo*. *Cell Cycle* **8,** 2802–2809
30. Sekine, S., Gutiérrez, P. J., Lan, B. Y., Feng, S., and Hebrok, M. (2007) Liver-specific loss of beta-catenin results in delayed hepatocyte proliferation after partial hepatectomy. *Hepatology* **45,** 361–368
31. Nejak-Bowen, K., and Monga, S. P. (2008) Wnt/beta-catenin signaling in hepatic organogenesis. *Organogenesis* **4,** 92–99
32. Tan, X., Behari, J., Cieply, B., Michalopoulos, G. K., and Monga, S. P. (2006) Conditional deletion of beta-catenin reveals its role in liver growth and regeneration. *Gastroenterology* **131,** 1561–1572
33. Nejak-Bowen, K. N., Thompson, M. D., Singh, S., Bowen, W. C., Jr., Dar, M. J., Khillan, J., Dai, C., and Monga, S. P. (2010) Accelerated liver regeneration and hepatocarcinogenesis in mice overexpressing serine-45 mutant beta-catenin. *Hepatology* **51,** 1603–1613
34. Cadoret, A., Ovejero, C., Terris, B., Souil, E., Lévy, L., Lamers, W. H., Kitajewski, J., Kahn, A., and Perret, C. (2002) New targets of beta-catenin signaling in the liver are involved in the glutamine metabolism. *Oncogene* **21,** 8293–8301
35. Yu, M., Gipp, J., Yoon, J. W., Iannaccone, P., Walterhouse, D., and Bushman, W. (2009) Sonic hedgehog-responsive genes in the fetal prostate. *J. Biol. Chem.* **284,** 5620–5629
36. Lamanna, W. C., Baldwin, R. J., Padva, M., Kalus, I., Ten Dam, G., van Kuppevelt, T. H., Gallagher, J. T., von Figura, K., Dierks, T., and Merry, C. L. (2006) Heparan sulfate 6-O-endosulfatases: discrete *in vivo* activities and functional co-operativity. *Biochem. J* **400,** 63–73
37. Farooqi, A. A., Mukhtar, S., Riaz, A. M., Waseem, S., Minhaj, S., Dilawar, B. A., Malik, B. A., Nawaz, A., and Bhatti, S. (2011) Wnt and SHH in prostate cancer: trouble mongers occupy the TRAIL towards apoptosis. *Cell. Prolif.* **44,** 508–515
38. Wilson, N. H., and Stoeckli, E. T. (2012) Sonic Hedgehog regulates Wnt activity during neural circuit formation. *Vitam. Horm.* **88,** 173–209
39. Bertrand, F. E., Angus, C. W., Partis, W. J., and Sigounas, G. (2012) Developmental pathways in colon cancer: crosstalk between WNT, BMP, Hedgehog and Notch. *Cell Cycle* **11,** 4344–4351